



ELSEVIER

Available online at [www.sciencedirect.com](http://www.sciencedirect.com)

ScienceDirect

journal homepage: [www.elsevier.com/locate/hydro](http://www.elsevier.com/locate/hydro)

## Egg-shell CuO/CeO<sub>2</sub>/Al<sub>2</sub>O<sub>3</sub> catalysts for CO preferential oxidation

Fernando Mariño<sup>a,\*</sup>, Ignacio Iglesias<sup>a</sup>, Graciela Baronetti<sup>a</sup>,  
Luis Alemany<sup>b</sup>, Miguel Laborde<sup>a</sup>

<sup>a</sup> ITHES (CONICET/Universidad de Buenos Aires), Laboratorio de Procesos Catalíticos, Pabellón Industrias, Ciudad Universitaria, 1428 Buenos Aires, Argentina

<sup>b</sup> Departamento de Ingeniería Química, Facultad de Ciencias, Campus de Teatinos, Universidad de Málaga, Málaga E-29071, Spain

### ARTICLE INFO

#### Article history:

Received 12 December 2014

Received in revised form

3 March 2015

Accepted 11 March 2015

Available online 1 April 2015

#### Keywords:

COPROX

Hydrogen

Intraparticle profiles

Copper

Cerium

### ABSTRACT

Catalytic systems based on copper and cerium supported on  $\gamma$ -Al<sub>2</sub>O<sub>3</sub> have shown to be extremely effective for CO preferential oxidation. In order to selectively oxidize carbon monoxide, it is desired that only CO can access to the active sites. Since the effective diffusion of H<sub>2</sub> is higher than that of CO, an egg-shell type distribution is preferred. With the objective of modifying the radial distribution of the active phases in the catalyst particle, the effect of four variables of the impregnation process is analyzed: metal loading, support-solution contact time, impregnation temperature and drying time. Radial profiles of Cu and Ce show that the egg-shell type distribution is favored by low metal loading, short contact and drying times and by high impregnation temperature. The effect of such variables is stronger on copper profile than on cerium profile. Catalytic performance on COPROX was enhanced by egg-shell type distribution.

Copyright © 2015, Hydrogen Energy Publications, LLC. Published by Elsevier Ltd. All rights reserved.

### Introduction

In view of the continuous increase in energy demand and environmental problems, the search for green energy sources has become imperious. When it is obtained from a renewable resource, hydrogen is a clean energy carrier that may overcome this challenge [1,2]. Its use in a PEMFC (Proton Exchange Membrane Fuel Cell) produces electricity with high efficiency and water as the only sub-product. In addition, PEMFC is foreseen as the most promising technology to replace combustion engines in mobile applications, primarily because of

their low operation temperature (80 °C) which allows fast startup [3–5].

Gaseous hydrogen may be obtained by steam reforming of bio-ethanol (SRE) typically using supported nickel catalysts operating at 700 °C. Carbon monoxide produced in SRE is a severe poison for platinum PEMFC anodes. As a consequence, the hydrogen stream produced requires subsequent purification. Among several alternatives, this purification could be carried out by means of two catalytic reactions: water gas shift – WGS – and carbon monoxide preferential oxidation - COPROX [6–8]. COPROX reaction system can be described by the following two chemical equations:

\* Corresponding author. Tel./fax: +54 1145763241.

E-mail address: [fernando@di.fcen.uba.ar](mailto:fernando@di.fcen.uba.ar) (F. Mariño).

<http://dx.doi.org/10.1016/j.ijhydene.2015.03.051>

0360-3199/Copyright © 2015, Hydrogen Energy Publications, LLC. Published by Elsevier Ltd. All rights reserved.



Therefore, a good COPROX catalyst should be able to oxidize as much CO as possible (favor Reaction 1) without consuming much hydrogen (avoid Reaction 2). For several years, copper–cerium catalytic system has been studied as a suitable alternative for this purpose [9–11].

Among different preparation procedures, impregnation of copper and cerium in a preformed support appears as the easiest to carry out at pilot plant scale operation. However, when this preparation method is employed, impregnation conditions may result in very different active phase profiles inside a support which in turn modify reactor performance [12].

Optimal distribution of catalytic phase in a support will depend on the reaction system and the fluid phase properties (composition, temperature and pressure). However, one should expect active phase uniform distributions to be more convenient when mass and heat transfer resistances have been removed. On the contrary, egg-shell profiles (active phase located near the support surface) should be preferred when diffusional resistances are dominant [13].

Taking into account that COPROX oxidation reactions are fast and that mass transfer resistances are relevant at pilot plant scale, egg-shell distribution of copper appears to be the most adequate [14]. Furthermore, since hydrogen effective diffusivity is considerably larger than that of carbon monoxide, egg-shell distribution should also favor selectivity towards CO oxidation [15]. It should also be noted that, being high temperature detrimental for COPROX selectivity, egg-shell more effective heat transference also favors our purpose.

In this work, we study the influence of impregnation conditions – copper loading, impregnation time and temperature, drying and calcination time – in the intraparticle copper distribution and its effect on the catalytic performance for COPROX – activity and selectivity towards CO<sub>2</sub>.

## Experimental

### Preparation of catalysts

γ-alumina spheres provided by Rhône-Poulenc ( $S_{\text{BET}} = 200 \text{ m}^2/\text{g}$ ,  $V_g = 0.44 \text{ ml/g}$ ,  $\phi = 3 \text{ mm}$ ) were used as support being their size, mechanical strength and thermal stability appropriate for operation in pilot plant scale. Catalysts were prepared by successive wet impregnation using metal nitrate salts as precursors (Aldrich) in concentrations as to get the desired

weight percentage of cerium and copper. Cerium content was either 10 wt% or 30 wt% while copper content was varied between 1 and 5 wt% (indicated as the first number in the sample name – see Table 1 and Table 2). Copper content effectively incorporated into the support was later determined by ICP (Shimadzu 9000).

Impregnation procedure was either carried out at ambient temperature or at 70 °C (differentiated by an ‘\*’ in sample name) while contact time used was 3 min or 6 h (distinction is made in letter ‘c’, being capital when contact time is large). In addition, some of the samples were dried overnight at 70 °C and then calcinated (ramp: 10 °C/min) while others were calcinated directly after impregnation (ramp: 20 °C/min) (following same logic that the one employed with contact time, letter ‘s’ in sample name is capital when large drying times were used). In all cases, the final calcination temperature was 450 °C, which was held for 5 h.

Preliminary activity tests using large contact and drying times, both for cerium and copper impregnation, were carried out for two purposes: i) evaluate the importance of mass transfer resistance with the chosen support and ii) search optimum loading values at this preparation conditions. In these experiments, cerium content was varied between 10 wt% and 30 wt% while copper content was varied between 1 and 5 wt%. Copper content is indicated as the first number in sample name and cerium content is 30 wt% unless otherwise indicated between parentheses. Samples prepared and conditions employed are summarized in Table 1.

For the study of copper profiles in CuO/CeO<sub>2</sub>/Al<sub>2</sub>O<sub>3</sub> catalysts, CeO<sub>2</sub>/Al<sub>2</sub>O<sub>3</sub> support preparation procedure was always the same: copper was impregnated on sample named Ce–C/S, except for catalyst named 1Cu–c/s # for which copper impregnation was made on CeO<sub>2</sub>/Al<sub>2</sub>O<sub>3</sub> sample named Ce–c/s. Samples prepared and conditions employed are summarized in Table 2.

### Metal profile determination

Catalyst spheres were cut in halves and metal profiles along the radial axis were determined by EDS (Zeiss Supra 4000). Atomic percentage was divided by its mean value in the catalyst volume and parameter sigma ( $\sigma$ ) was used for quantification of profile discrepancy with respect to a uniform one (Eq. (1)), similarly as defined by Lekhal et al. [16].

$$\sigma = \sum_{i=1}^N \frac{|m_i^* - 1|}{N} \quad (1)$$

N is number of discrete points where atomic percentage was determined and  $m_i^*$  is the dimensionless atomic percentage of the metal considered. It should be observed that, from this

**Table 1 – Samples prepared for preliminary tests.**

Sample	$t_{\text{Solution}}$ [min]	$T_{\text{Solution}}$ [°C]	$t_{\text{Drying}}$ [min]	$\text{Cu}_{\text{nominal}}$ [wt %]	$\text{Cu}_{\text{ICP}}$ [wt%]
1Cu–C/S (10)	360	25	720	1.0	0.84
1Cu–C/S	360	25	720	1.0	0.62
2.5Cu–C/S (10)	360	25	720	2.5	2.12
2.5Cu–C/S	360	25	720	2.5	1.74
5Cu–C/S (10)	360	25	720	5.0	4.22
5Cu–C/S	360	25	720	5.0	3.14

**Table 2 – Samples prepared for profile study and sigma parameter defined in Eq. (1).**

Sample	t <sub>Solution</sub> [min]	T <sub>Solution</sub> [°C]	t <sub>Drying</sub> [min]	Cu <sub>nominal</sub> [wt %]	Cu <sub>ICP</sub> [wt%]	σ <sub>Ce</sub>	σ <sub>Cu</sub>
Ce–C/S	360	25	720	–	–	0.05	–
Ce–c/S	3	25	720	–	–	0.08	–
Ce–C/s	360	25	0	–	–	0.45	–
Ce–c/s	3	25	0	–	–	0.64	–
Ce–C*/S	360	70	720	–	–	0.22	–
1Cu–c/s	3	25	0	1.0	0.26	0.05	1.03
1Cu–c/s <sup>#</sup>	3	25	0	1.0	0.51	0.64	1.05
2.5Cu–C/S	360	25	720	2.5	1.74	0.05	0.09
2.5Cu–C*/S	360	70	720	2.5	2.40	0.05	0.56
2.5Cu–c/S	3	25	720	2.5	0.66	0.05	0.13
2.5Cu–C/s	360	25	0	2.5	1.25	0.05	0.37
2.5Cu–c/s	3	25	0	2.5	0.81	0.05	0.78
2.5Cu–c*/s	3	70	0	2.5	1.29	0.05	1.33
5Cu–c/s	3	25	0	5.0	1.47	0.05	0.70

definition,  $\sigma$  will be zero for a uniform profile and takes increasing values for egg-shell type distributions. Values for  $\sigma_{Ce}$  and  $\sigma_{Cu}$  are tabulated in Table 2. In Section 3.3 and thereafter, results are presented as dimensionless metal profile ( $m_i^*$ ) versus dimensionless radius ( $r_i^*$ ).

### Activity tests

Activity tests were carried out in an isothermal tubular fixed bed reactor where temperature was measured by a K-type thermocouple placed at the center of the catalyst bed. High purity gases (AirLiquide) were fed by mass flow controllers (Aalborg). Gas mixture composition both at the entrance and the exit of the reactor was analyzed by gas chromatography employing a Shimadzu GC 14-B chromatograph equipped with TCD and FID detectors. Before each activity test, catalyst was pretreated with air at 250 °C for 30 min. Afterwards, temperature was lowered in steps to 100 °C registering exit gas composition at each temperature to calculate CO and O<sub>2</sub> conversions and selectivity towards CO<sub>2</sub> (Eqs. (2)–(4)). All catalytic tests were performed with constant residence time (0.09 g.s.cm<sup>-3</sup>) and the following composition at reactor entrance: CO (1%), H<sub>2</sub> (79%), O<sub>2</sub> (0.85%) and N<sub>2</sub> (as balance).

$$x_{CO} = \frac{F_{CO}^{in} - F_{CO}^{out}}{F_{CO}^{in}} \quad (2)$$

$$x_{O_2} = \frac{F_{O_2}^{in} - F_{O_2}^{out}}{F_{O_2}^{in}} \quad (3)$$

$$S = \frac{x_{CO}}{x_{O_2}} \frac{F_{CO}^{in}}{2F_{O_2}^{in}} \quad (4)$$

where  $F$  is the molar flow (inlet or outlet) of the considered compound.

## Results and discussion

### Mass transfer resistance

Preliminary activity tests were performed to check the importance of mass transfer resistances when using a 3 mm

support. For this purpose, a 5Cu–C/S catalyst was prepared using three different support sizes: 297–500 μm, 1.8 mm and 3 mm (see Table 1 for sample information).

As Fig. 1 shows, in the range of support sizes explored, maximum attainable CO conversion is substantially incremented with decreasing particle size which was expected in regards of internal and external mass transfer resistance. Therefore, to increase catalyst effectiveness in a 3 mm catalyst, egg-shell type distribution is justified.

### Metal content at large contact and drying times

As it will further explained in next sections, large contact and drying times ensure uniform metal distribution in the

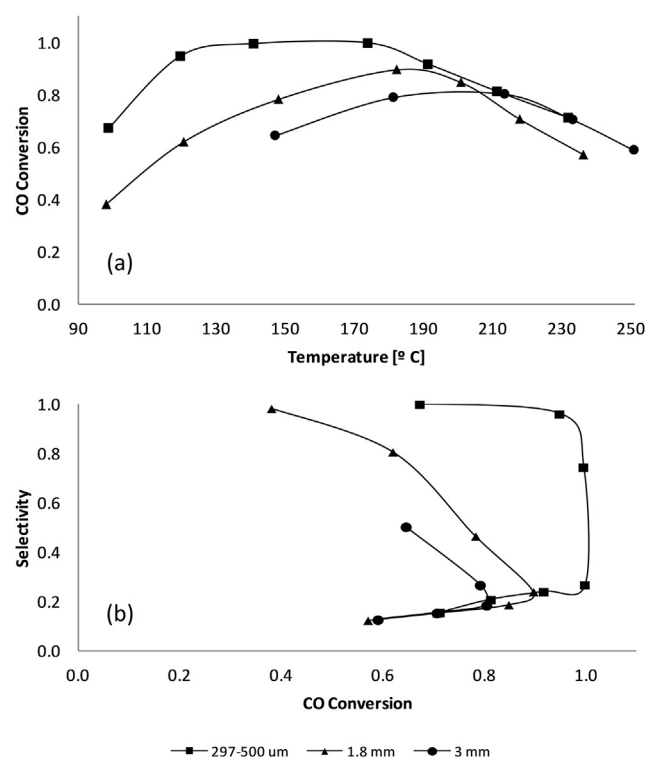


**Fig. 1 – Catalytic activity results for samples with different particle diameter. CO conversion (a) and Selectivity (b) are represented versus reaction temperature.**

support. For this simplified preparation conditions, copper and cerium content was varied to obtain a starting point for metal profiles study. Consequently, activity tests were performed with samples summarized in Table 1: copper content was varied between three different values (1 wt%, 2.5 wt% and 5 wt%) for every  $\text{CeO}_2/\text{Al}_2\text{O}_3$  support (cerium content was either 10 wt% or 30 wt%).

Fig. 2 shows that optimum copper loading surges of a balance between oxygen conversion and selectivity towards  $\text{CO}_2$ . High copper contents favor oxygen conversion since more active sites are expected but, on the other hand, large copper particles resulting from poor dispersion favor hydrogen oxidation causing a loss of selectivity.

In addition, it is seen that the higher the cerium content, the higher the selectivity towards CO oxidation. This result is in accordance with other results found in literature where copper–cerium intimate contact is identified as a key factor for ensuring COPROX selectivity [7].

Considering the results commented in this section, copper and cerium loadings of 2.5 wt% and 30 wt% respectively were chosen as start point for metal profiles study in search of an optimized egg-shell catalyst.

### Cerium profiles on $\text{CeO}_2/\text{Al}_2\text{O}_3$ samples

Fig. 3 shows the dimensionless cerium profiles inside the support for samples Ce–C/S, Ce–c/S, Ce–c/s and Ce–C/s. First, it is noteworthy that cerium profile for sample Ce–C/S is close to 1 all along catalyst radius indicating that an uniform

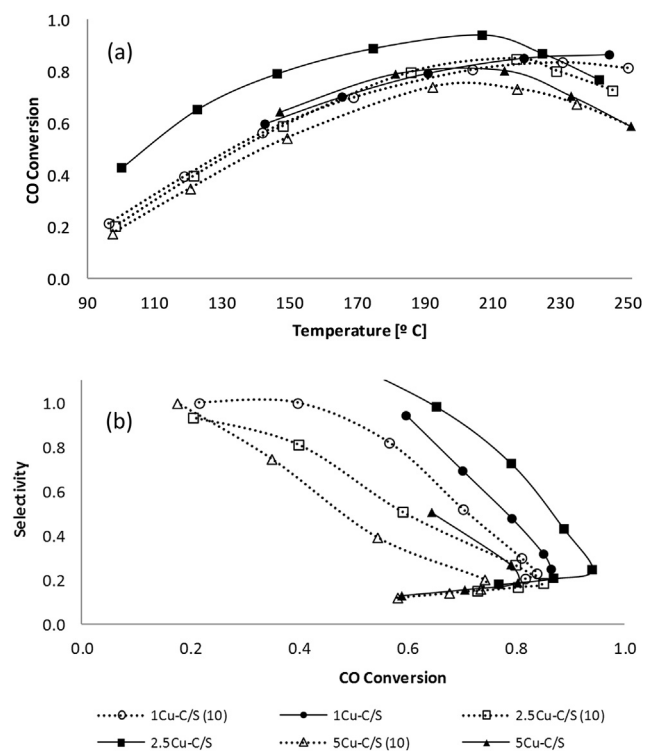


Fig. 2 – Catalytic activity results for samples for different copper and cerium content. CO conversion (a) and Selectivity (b) are represented versus reaction temperature.

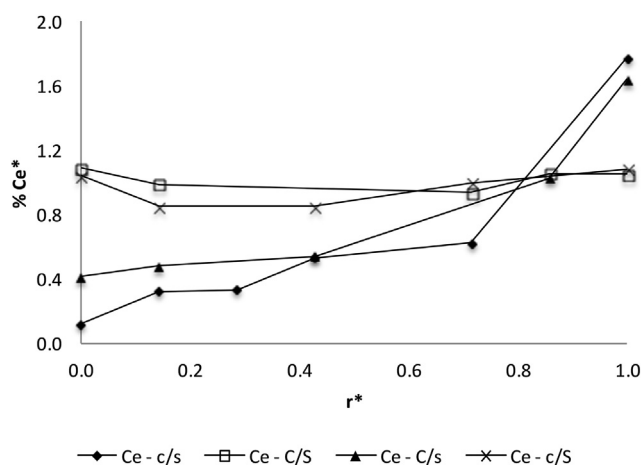


Fig. 3 – Cerium profiles with varying contact and drying time. Catalysts: Ce–c/s, Ce–C/S, Ce–C/s, Ce–c/S.

distribution was obtained (in fact,  $\sigma$  parameter is nearly zero in this case). Once impregnating solution filled the support pores, long impregnation times (360 min) allow diffusion processes to homogenize metal concentration. In addition, when drying was performed at moderate conditions (70 °C, 720 min) this profile does not change substantially.

Profiles in Fig. 3 also reveal that the impact of short drying times is stronger than that of short contact times with the objective of obtaining an egg-shell type distribution, as it is also reflected in  $\sigma$  values for these samples (see Table 2). When combining short impregnation and drying times (Ce–c/s sample), the highest values of  $\sigma$  are obtained, as expected.

In Fig. 4, sample Ce–C\*/S profile is plotted together with Ce–C/s and Ce–c/s profiles (already presented) for comparison. Results show that high temperature (70 °C) of the solution during impregnation step favors superficial distribution of cerium. Nevertheless,  $\sigma$  value for Ce–C\*/S sample is lower than that of Ce–c/s sample, confirming the greater effect of

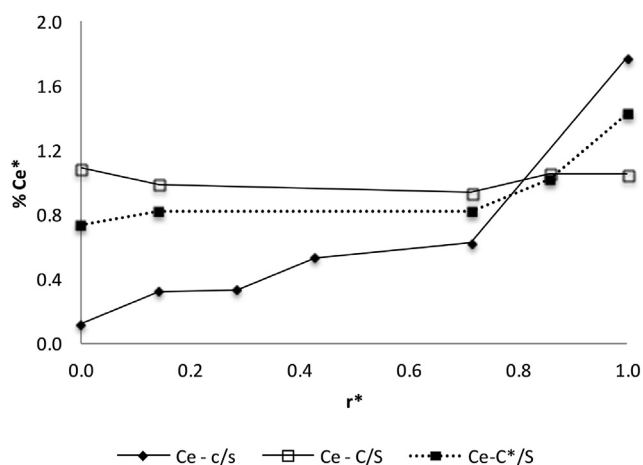


Fig. 4 – Impregnating solution temperature effect on cerium profile. Catalysts: Ce–c/s, Ce–C/S, Ce–C\*/S.

drying time on the resulting Ce profile (see Table 2). Increasing solution temperature during impregnation lowers its viscosity which in turn enhances convective transport inside the support being cerium ions retarded on the catalyst surface [17].

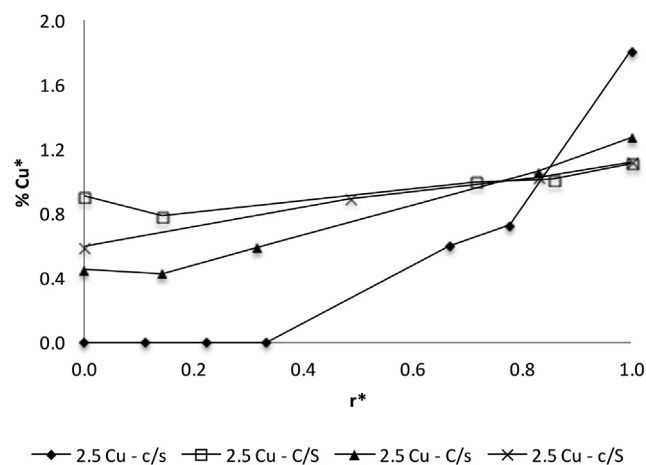
### Copper profiles on CuO/CeO<sub>2</sub>/Al<sub>2</sub>O<sub>3</sub> samples

Fig. 5 shows the dimensionless copper profiles inside the sphere for the 2.5 wt% copper samples: 2.5Cu–C/S, 2.5Cu–c/S, 2.5Cu–c/s and 2.5Cu–C/s. As observed for cerium in Fig. 3, copper profile for sample 2.5Cu–C/S is close to 1 all along catalyst radius indicating an uniform distribution. Again, similarly to cerium behavior, copper profiles in Fig. 5 show that the effect of drying time is more significant than that of contact time. Compared to cerium profiles, the effect of drying and contact times is greater in the case of copper, as it can be confirmed by the  $\sigma$  values reported in Table 2. In addition, it should be remarked that no copper is encountered in the inner part of the sphere for 2.5Cu–c/s sample (Cu atomic percentage is zero for  $r^* \leq 0.3$ ).

Fig. 6 shows the effect of increasing the solution temperature during copper impregnation for two different samples: 2.5Cu–C/S (the one with lowest  $\sigma$  value) and 2.5Cu–c/s (the one with highest  $\sigma$  value). Copper profiles for 2.5Cu–C\*/S and 2.5Cu–c\*/s show that impregnation at 70 °C have favored the generation of sharp profiles near the surface (high  $r^*$  values) with respect to the same samples impregnated at room temperature.

Once that short contact and drying times have been identified as key conditions for obtaining egg-shell type catalysts, copper loading was varied between 1 and 5% wt% to analyze the influence of this variable on copper profiles. Fig. 7 and Table 2 show that  $\sigma$  values increase as copper concentration decreases, which can be explained by a lower driving force for diffusion process [18].

In addition, Fig. 7 shows the copper profile determined for sample named 1Cu–c/s<sup>#</sup>, which has the same copper impregnation procedure as 1Cu–c/s sample, but differs in the CeO<sub>2</sub>/Al<sub>2</sub>O<sub>3</sub> support used ( $\sigma_{Ce} = 0.64$  for 1Cu–c/s<sup>#</sup> and  $\sigma_{Ce} = 0.05$



**Fig. 5 – Copper profiles with varying contact and drying time. Catalysts: 2.5Cu–c/s, 2.5Cu–C/S, 2.5Cu–C/s, 2.5Cu–c/S.**

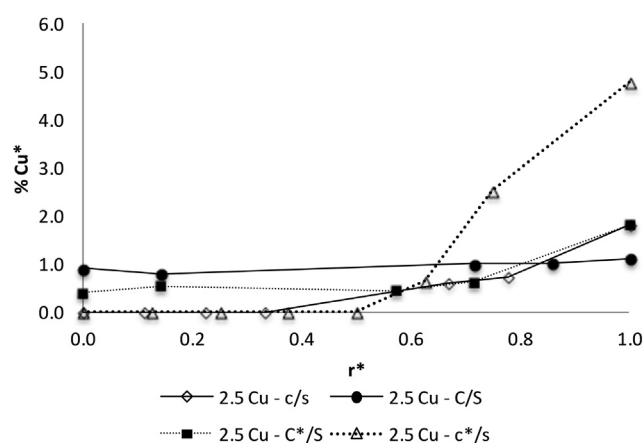


**Fig. 6 – Impregnating solution temperature effect on copper profile. Catalysts: 2.5Cu–c/s, 2.5Cu–C/S, 2.5Cu–C\*/S, 2.5Cu–c\*/s.**

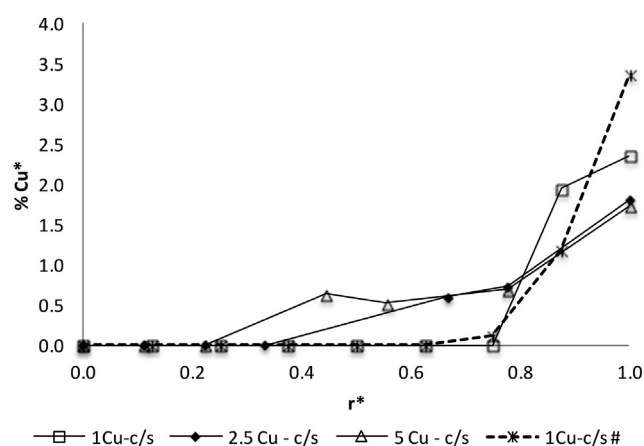


**Fig. 7 – Copper profiles with varying metal loading. Catalysts: 1Cu–c/s, 2.5Cu–c/s, 5Cu–c/s, 1Cu–c/s<sup>#</sup>.**

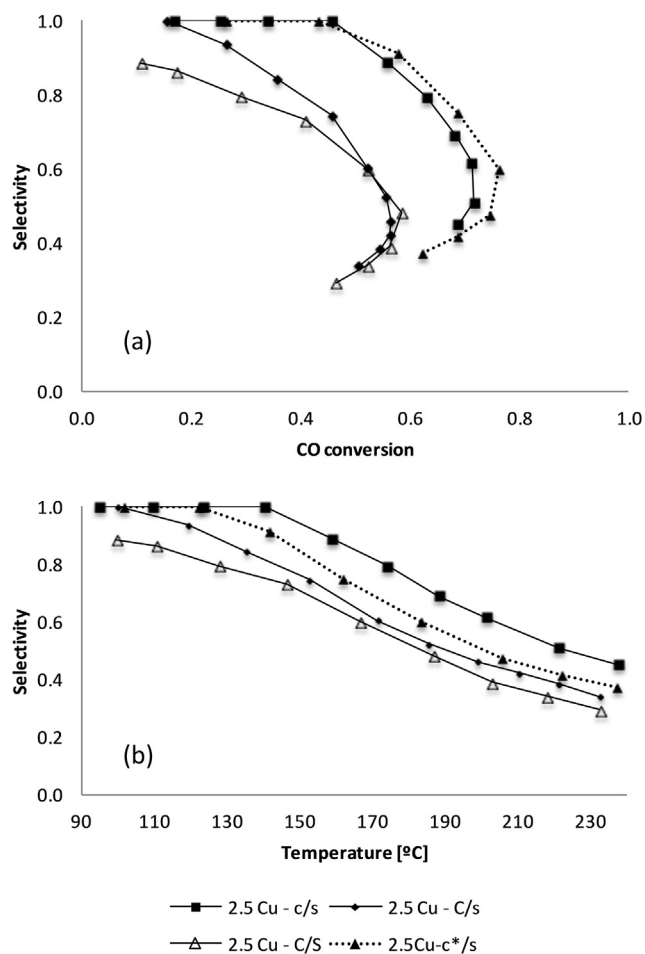
for 1Cu–c/s). As it can be seen, copper profiles and  $\sigma$  values for both samples are practically the same (see Fig. 7 and Table 2).

Regarding the copper loading effectively incorporated into the catalyst, results in Table 2 show that copper content is always below nominal value. Reduced impregnation and drying times result in copper contents even lower [19]. On the other hand, increasing solution temperature results in increased metal loading because of the enhanced solution transport mentioned previously. Finally, when comparing samples 1Cu–c/s and 1Cu–c/s<sup>#</sup>, it is observed that copper is more easily incorporated on the sample with highest cerium sigma value (short impregnation and drying time). This is explained by taking into account that high cerium content (nominal value: 30 wt%) combined with long impregnation and drying times in sample 1Cu–c/s probably produce some pore blockage which inhibits subsequent copper incorporation.

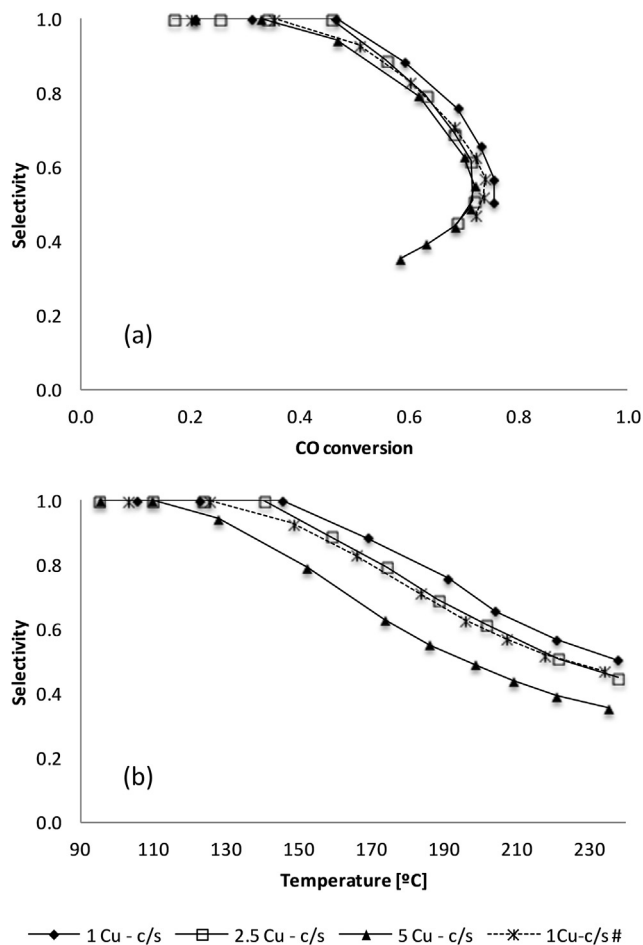
### Catalytic activity

Fig. 8 shows selectivity towards CO<sub>2</sub> versus CO conversion (a) and temperature (b) for four different catalysts: 2.5Cu–C/S ( $\sigma = 0.09$ ), 2.5Cu–C/s ( $\sigma = 0.37$ ), 2.5Cu–c/s ( $\sigma = 0.78$ ) and 2.5Cu–c\*/s ( $\sigma = 1.33$ ). Except for sample named 2.5Cu–c\*/s, selectivity at any temperature increases with sigma value which is in accordance with theoretical considerations previously made. The exception found for 2.5Cu–c\*/s sample is explained in terms of copper segregation, since the high  $\sigma$  value obtained for this catalyst in addition to its higher metal loading may have resulted in copper aggregates which are known to favor hydrogen oxidation [20]. Nevertheless, it should be observed that this catalyst is the one that approximates the most to optimum performance located at the top right corner of the Selectivity vs. Conversion plot (complete CO conversion with 100% selectivity).

Fig. 9 presents the same results for varying copper loading (copper profiles for this samples are shown in Fig. 7). The most suitable balance between CO conversion and selectivity is achieved for catalyst 1Cu–c/s. Regarding catalyst 1Cu–c/s#, it is seen in Fig. 9 that it has lower selectivity than 1Cu–c/s



**Fig. 8 – Catalytic activity results for indicated samples. Selectivity is represented versus carbon monoxide conversion (a) and temperature (b).**



**Fig. 9 – Catalytic activity results for indicated samples. Selectivity is represented versus carbon monoxide conversion (a) and temperature (b).**

probably due to a lower cerium content resulting from short impregnation time.

### Conclusions

Mass transfer resistances were proven to be relevant in a spherical 3 mm  $\gamma$ -Al<sub>2</sub>O<sub>3</sub> support justifying this study.

Wet impregnation conditions were varied to obtain different copper and cerium distributions in the support mentioned. It was shown that high impregnation and drying times led to uniform distributions. With this preparation conditions, copper and cerium loadings were optimized (2.5 wt% and 30 wt%, respectively) and taken as starting point for deeper investigation.

It was shown that short impregnation and drying times, low solution concentrations and high solution temperature during impregnation favor egg-shell type distributions. Furthermore, it was seen that copper egg-shell type distribution is better achieved on a uniformly cerium impregnated support.

Catalysts prepared were tested in COPROX system where egg-shell type distributions demonstrated to have better activity and selectivity when comparing them to uniform ones.

---

## Acknowledgments

The authors acknowledge to the University of Buenos Aires (UBA), ANPCyT and CONICET for their financial support.

---

## REFERENCES

- [1] Dincer I. Environmental and sustainability aspects of hydrogen and fuel cell systems. *Int J Energy Res* 2007;31:29–55.
- [2] Turner J, Sverdrup G, Mann MK, Maness PC, Kroposki B, Ghirardi M, et al. Renewable hydrogen production. *Int J Energy Res* 2008;32:379–407.
- [3] Ghenciu AF. Review of fuel processing catalysts for hydrogen production in PEM fuel cell systems. *Curr Opin Solid State Mater Sci* 2002;6:389–99.
- [4] U.S. Department of Energy. Fuel cell handbook. 7th ed. EG&G Technical Services, Inc.; 2004.
- [5] Yee RSL, Rozendal RA, Zhang K, Ladewiga BP. Cost effective cation exchange membranes: a review. *Chem Eng Res Des* 2012;90:950–9.
- [6] Oh SH, Sinkevitch RM. Carbon monoxide removal from hydrogen-rich fuel cell feedstreams by selective catalytic oxidation. *J Catal* 1993;142:254–62.
- [7] Avgouropoulos G, Ioannides T, Papadopoulou Ch, Batista J, Hocevar S, Matralis HK. A comparative study of Pt/ $\gamma$ -Al<sub>2</sub>O<sub>3</sub>, Au/ $\alpha$ -Fe<sub>2</sub>O<sub>3</sub> and CuO–CeO<sub>2</sub> catalysts for the selective oxidation of carbon monoxide in excess hydrogen. *Catal Today* 2002;75:157–67.
- [8] Mishra A, Prasad R. A review on preferential oxidation of carbon monoxide in hydrogen rich gases. *Bull Chem React Eng Catal* 2011;6:1–14.
- [9] Mariño F, Descorme C, Duprez D. Supported base metal catalysts for the preferential oxidation of carbon monoxide in the presence of excess hydrogen (PROX). *Appl Catal B Environ* 2005;58:175–83.
- [10] Bion N, Epron F, Moreno M, Mariño F, Duprez D. Preferential oxidation of carbon monoxide in the presence of hydrogen (PROX) over noble metals and transition metal oxides: advantages and drawbacks. *Top Catal* 2008;51:76–88.
- [11] Schönbrod B, Mariño F, Baronetti G, Laborde M. Catalytic performance of a copper-promoted CeO<sub>2</sub> catalyst in the CO oxidation: Influence of the operating variables and kinetic study. *Int J Hydrogen Energy* 2009;34:4021–8.
- [12] Augustine RL. Heterogeneous catalysis for the synthetic chemist. Marcel Dekker, Inc; 1996.
- [13] Morbidelli M, Gavriilidis A, Varma A. Catalyst design: optimal distribution of catalyst in pellets, reactors and membranes. Cambridge University Press; 2001.
- [14] Potemkin DI, Snytnikov PV, Belyaev VD, Sobyenin VA. Preferential CO oxidation over Cu/CeO<sub>2</sub>-x catalysts: internal mass transport limitation. *Chem Eng J* 2011;177:165–71.
- [15] Vayenas CG, Pavlou S. Optimal catalyst distribution for selectivity maximization in pellets: parallel and consecutive reactions. *Chem Eng Sci* 1987;42:1655–66.
- [16] Lekhal A, Glasser BJ, Khinast JG. Impact of drying on the catalyst profile in supported impregnation catalyst. *Chem Eng Sci* 2001;56:4473–87.
- [17] Kötter M, Riekert L. The influence of impregnation, drying and activation on the activity and distribution of CuO on  $\alpha$ -alumina. *Stud Surf Sci Catal* 1979;3:51–63.
- [18] Liu X, Khinast JG, Glasser BJ. Drying of supported catalysts for low melting point precursors: impact of metal loading and drying methods on the metal distribution. *Chem Eng Sci* 2012;79:187–99.
- [19] Liu X, Khinast JG, Glasser BJ. A parametric investigation of impregnation and drying of supported catalyst. *Chem Eng Sci* 2008;63:4517–30.
- [20] Mariño F, Baronetti G, Laborde M, Bion N, Le Valant A, Epron F, et al. Optimized CuO–CeO<sub>2</sub> catalysts for COPROX reaction. *Int J Hydrogen Energy* 2008;33:1345–53.